CrossMark

Temporal Evolution of Solar Energetic Particle Spectra

Donald J. Doran[1] · Silvia Dalla[1]

Abstract During solar flares and coronal mass ejections, Solar Energetic Particles (SEPs) may be released into the interplanetary medium and near-Earth locations. The energy spectra of SEP events at 1 AU are typically averaged over the entire event or studied in a few snapshots. In this article we analyze the time evolution of the energy spectra of four large selected SEP events using a large number of snapshots. We use a multi-spacecraft and multi-instrument approach for the observations, obtained over a wide SEP energy range. We find large differences in the spectra at the beginning of the events as measured by different instruments. We show that over time, a wave-like structure is observed traveling through the spectra from the highest energies to the lowest energies, creating an "arch" shape that then straightens into a power law later in the event, after times on the order of 10 hours. We discuss the processes that determine SEP intensities and their role in shaping the spectral time evolution.

Keywords Solar Energetic Particles · Particle energy spectra · Solar activity

1. Introduction

Solar Energetic Particles (SEPs) are ions and electrons that have been accelerated from the coronal and solar wind plasma by solar flares and coronal mass ejections (CMEs). SEP ions consist mainly of protons, with additional small numbers of heavier ions from helium up to iron, and even heavier species. SEPs are of particular importance for scientific and space exploration missions because they are a radiation hazard to spacecraft and to human occupants. Of these radiation hazard particles, protons are the most abundant, and therefore present the most serious safety risk. In this regard, human occupants can suffer cumulative radiation dosages causing serious health issues, and spacecraft can experience irreversible damage to their functional electronics (Crosby, Heynderickx, and Jiggens, 2013).

✉ S. Dalla
sdalla@uclan.ac.uk

[1]   University Central Lancashire, Preston, UK

SEP events are typically studied by analyzing the profiles of particle intensity versus time. Multi-spacecraft observations have elucidated how SEP profiles and their properties depend on the location of the observing spacecraft with respect to the associated solar events (Cane, Reames, and von Rosenvinge, 1988; Kallenrode *et al.*, 1993; Reames, Barbier, and Ng, 1996; Richardson *et al.*, 2014). It is well known that near-Earth spacecraft are magnetically connected to solar locations on the western limb, therefore events within $W20 - W80$ have the highest probability to produce SEP events at Earth. The role of latitudinal separation between observers and solar source regions in determining whether or not an SEP event will be observed is less clear (Dalla and Agueda, 2010).

The long-standing interpretation of the transport of SEPs from the corona through the heliosphere has assumed propagation to be along the interplanetary magnetic field (IMF) lines, without transport of particles perpendicular to the field. When particles are accelerated by CME-driven shocks, the region of injection is very extended, providing a possible explanation for the fact that SEPs are often observed by spacecraft at large longitudinal separation from the source active region at the Sun. However, recent observations of impulsive SEP events by widely separated spacecraft (Wiedenbeck *et al.*, 2013) seem to imply significant cross-field transport, or movement across the interplanetary magnetic field lines, since for this type of event, the injection is thought to take place in a relatively compact flare region. Dresing *et al.* (2014) analyzed a number of SEP events observed by STEREO and concluded that one possible mechanism for the wide-spread type SEP event is efficient perpendicular transport in the interplanetary medium (IM), while another scenario is a wide particle spreading occurring close to the Sun, and probably both mechanisms are at work for many SEP events. Of the possible mechanisms for transport across the field, recent work has shown that drifts due to the gradient and curvature of the interplanetary magnetic field are significant (Marsh *et al.*, 2013). Drift takes place in both scatter-free and scattering modes and is a function of particle energy as well as the location of the particle source at the Sun (Dalla *et al.*, 2013; Kelly, Dalla, and Laitinen, 2012). Drift of SEPs also produces deceleration because particles move anti-parallel to the solar wind electric field, a process that has been termed drift-induced deceleration (Kóta, 1979; Dalla, Marsh, and Laitinen, 2015).

Energy spectra, showing the particle intensity at a given time versus the average energy of each instrument channel, provide an alternative view of SEP events. Although spectra have been analyzed for a variety of SEP events, in most studies a single representative spectrum is shown for an entire event. Event-integrated spectra tend to exhibit a power-law dependence, which for large shock-associated gradual events almost always yields a double power law, sometimes called a knee. According to Li *et al.* (2009), the energy break or rollover feature depends on $(Q/A)^\alpha$, where Q is the ionic charge and A is the ion mass in atomic mass units, with the power-law index α ranging between ≈ 1 and ≈ 2. The Q/A dependence of the break energies, however, is not always easy to determine because the charge state is very often uncertain. Mewaldt *et al.* (2012) presented event-integrated proton spectra for 16 GLE events over an energy range from 0.3 MeV to ≈ 700 MeV.

Reames, Kahler, and Ng (1997) considered energy spectra at three times during an SEP event observed by multiple spacecraft and showed that so-called invariant spectra are observed in the decay phase of the event, where the different spectra of each observing spacecraft become very similar to each other. A new approach to the time evolution of the energy spectra of SEPs was proposed by Laurenza *et al.* (2012). The authors used the Shannon differential entropy to study the time evolution of a particle event measured by the SOHO ERNE instrument in the proton energy range of $1.67 - 112$ MeV.

In this article we analyze the time evolution of SEP spectra using a large number of snapshots and instrumentation from multiple spacecraft. We consider data for some historical events that took place in the 1970s as well as more recent events observed by STEREO.

Our focus is on large events with strong flux at both the low- and high-energy ends of the SEP range, to ensure that many spectral points with good statistics are available. We discuss the observations within the framework of the current understanding of SEP acceleration and propagation. We also discuss spectral indices for these events, comparing the event-averaged spectra with those late in the event after the spectral break when the arch structure is no longer present in the spectra.

2. Observations

The types of data to be used for this project include various previously compiled lists of SEP events and actual data collected by a variety of spacecraft. The type of events of particular interest are those with high flux at the low-energy channels, *e.g.* 5 – 15 MeV, and having at the same time high flux at the high-energy channels, *e.g.* > 100 MeV. In this article we focus on SEP protons using nine spacecraft and their instruments, as highlighted below and also detailed in Table 1:

- ACE (*Advanced Composition Explorer*), with the instruments ULEIS (*Ultra Low Energy Isotope Spectrometer*, 0.6 to 8.7 MeV/n energy range) and SEPICA (*Solar Energetic Particle Ionic Charge Analyzer*, 0.4 to 6.0 MeV/n energy range) at the website http://www.srl.caltech.edu/ACE/. See Stone *et al.* (1998).
- GOES 11 and 13 (*Geostationary Operational Environment Satellites*), with the instruments SEM/ESP (*Space Environment Monitor and Energetic Particle Sensor*) at the website www.swpc.noaa.gov/Data/goes.html. See Onsager *et al.* (1996), McCuistion and Bengston (1996).
- HELIOS 1 and 2, E6 experiment, *Energetic Electron and Proton Detector* (low-energy telescope at 4 – 51 MeV/n energy range), and E7 experiment (high-energy telescope at 3.4 – 206.5 MeV energy range), at the website http://nssdc.gsfc.nasa.gov/nmc/spacecraftDisplay. See Porsche (1981).
- IMP-8 GME (*Goddard Medium Energy Experiment*), also called *Explorer 50*, and IMP-J at the website http://spdf.gsfc.nasa.gov/imp8/GME, and CRNC (*Cosmic Ray Nuclear Composition Experiment*) at the web site http://explorers.gsfc.nasa.gov/missions.html.
- SOHO (*The Solar and Heliospheric Observatory*) ERNE (*Energetic and Relativistic Nuclei and Electron experiment*) at the websites http://soho.esac.esa.int/data/data.html or http://soho.nascom.nasa.gov/about/about.html. See Torsti *et al.* (1995).
- STEREO A (ahead of Earth) and STEREO B (behind Earth) (*Solar TErrestrial RElations Observatory*), the IMPACT instrument (*In-situ Measurement of Particles and CME Transients*), LET (*Low Energy Telescope*), See Mewaldt *et al.* (2008), and HET (*High Energy Telescope*), See von Rosenvinge *et al.* (2008) at the website http://www.nasa.gov/mission-pages/stereo/main/index.html.
- WIND (*Comprehensive Solar Wind Laboratory for Long Term Solar Wind Measurements*), the 3DP SST instrument (*3 Dimensional Plasma Analyzer Solid State Telescope*) measuring protons up to 6 MeV/n, at the website http://wind.nasa.gov/, see Lin *et al.* (1995).

The observational data have been obtained over diverse locations in space, as shown in Table 1, from the near-Earth geocentric views of IMP-8, to HELIOS 1 and 2 orbiting the Sun, to SOHO and ACE just outside the Earth's magnetosphere, and with those of GOES 11 and 13 as well as WIND inside the Earth's magnetosphere, and finally to the stereoscopic views of STEREO A and B. Several different space environments are observed by the IMP-8

Table 1 Spacecraft and instruments used for data acquisition.

Spacecraft	Instrument	Proton Energy, MeV	Start Date	End Date	Orbit
ACE	SEPICA	0.4 – 6.0	Aug 1997	active	L1
ACE	ULEIS	0.6 – 8.7	Aug 1997	active	L1
GOES 11	ESP	0.6 – 500	May 2000	Dec 2011	Geostationary
GOES 13	ESP	0.7 – 500	Jun 2006	active	Geostationary
HELIOS 1	E6	4.0 – 51.0	Jan 1975	Feb 1985	Heliocentric
HELIOS 1	E7	3.4 – 206.5	Jan 1975	Feb 1985	Heliocentric
HELIOS 2	E6	4.0 – 51.0	Jul 1976	Dec 1979	Heliocentric
HELIOS 2	E7	3.4 – 206.5	Jul 1976	Dec 1979	Heliocentric
IMP-8	CRNC	10.9 – 95.0	Oct 1973	active	Geostationary
IMP-8	GME	0.9 – 237	Oct 1973	active	Geostationary
SOHO	ERNE	1.8 – 50.7	Dec 1995	active	L1
STEREO A	LET	1.8 – 15.0	Oct 2006	active	Heliocentric
STEREO A	HET	13.6 – 100	Oct 2006	active	Heliocentric
STEREO B	LET	1.8 – 15.0	Oct 2006	active	Heliocentric
STEREO B	HET	13.6 – 100	Oct 2006	active	Heliocentric
WIND	3DP-SST	0.1 – 6	Nov 1994	active	L1 now L2

Table 2 Properties of solar events associated with the four studied SEP events, showing the start times of the flare and CME, not the start time of the event, and with NAR being the NOAA active region number.

No.	Event Date	Flare/CME start time	Type	Location	NAR	X-ray class
1	1977-11-22	21:30	flare	N23W40		X1
2a	2000-07-14	10:03	flare	N22W07	9077	X5.7
2b	2000-07-14	10:54	CME	N20W08		halo
3a	2001-04-15	13:19	flare	S20W85	9415	X14.7
3b	2001-04-15	14:06	CME	S20W90		halo
4a	2012-03-07	02:00	flare	N17E15	11429	X5.7
4a	2012-03-07	00:24	CME	N22E12		halo

instruments as the spacecraft passes through the bow shock, magnetosphere, magnetotail, and the solar wind in its geocentric orbit of 25 to 45 Earth radii. In each orbit of 12.5 days, it spends only seven–eight days in the solar wind, but nevertheless provides much-needed information on particle flux at the near-Earth position.

Four widely different SEP events have been examined, starting with their individual time-intensity plots, and followed by a study of the time evolution of their spectra. The first of these events is associated with a single flare (No. 1 of Table 2), but there may also have been a CME since there were no CME observations in 1977. The second event is due to both a CME and an associated flare (Nos. 2a and 2b of Table 2). The third event is a complicated series of four CMEs and associated flares (Nos. 3a and 3b), but we focus on the third peak of Figure 9. Finally, the fourth and last event is a series of two CMEs and associated flares (Nos. 4a and 4b), but we focus on peak A of Figure 14.

3. Selection of SEP Events for Study

We selected four SEP events among those with an intensity $> 10^2$ as measured in particles $cm^{-2} s^{-1} sr^{-1} (MeV/nuc)^{-1}$ in the $10 - 15$ MeV energy channel as well as 0.1 intensity in the $138 - 200$ MeV channel, over the time range of $1976 - 2012$. A further criterion was added: the time-intensity profile of the event should resemble the so-called classic profile whereby the particle flux rises sharply, followed by a steady and even decay over a period of two to four days. It was necessary to apply this requirement as some of the events selected for study, although very intensive and energetic, were nevertheless very complex in their profiles, with several spikes and irregularities in their decays. A final list of 14 events satisfied the above selection criteria during 1976 to 2012, and of these, four were chosen for detailed study.

The time-intensity profiles for a near-Earth observer for the selected events were obtained from ESA's *Solar Energetic Particle Environment Modeling* (SEPEM) application server (Crosby *et al.*, 2015). This server uses data compiled from the IMP-8/GME and the GOES 7-13/SEM/EPS instruments covering the period November 1973 to March 2012 to generate the so-called SEPEM reference proton data set. The advantage of using the dataset is that the SEP fluxes have been inter-calibrated and de-spiked, producing a uniform dataset. In addition, the SEPServer data server was used for the HELIOS 1 and 2, STEREO A/B, and SOHO/ERNE plots (Vainio *et al.*, 2013).

Spectra were plotted with a resolution of 1 to 2 hours over the course of the event. Spectral plots were made using *The Virtual Energetic Particle Observatory* (VEPO) analysis tool, which operates within the domain of the *Virtual Heliospheric Observatory* (VHO). VEPO has two interfaces for generating spectral plots of energetic particle fluxes from multiple instruments flown on multiple spacecraft. The fluxes are averaged over user-specified time spans. We used the Multi-Source Spectral Plots-1, (MSSP-1), which provides spectral plots of H and He for 30 data sources.

4. Results and Data: Time-Intensity and Spectral Plots of Four Selected SEP Events

4.1. GLE Event of 1977-11-22

The event of 1977-11-22 dates back to the early history of SEP investigations, and although there are no data from the SolarMonitor, CDAW, or HELIO catalogs, all the literature publications seem to agree on the flare identification of the event. This is clearly the only strong SEP event for the month of November 1977, making it a good choice for the study of its properties without interference from preceding or following flares or CMEs. The time-intensity profile is shown in Figure 1, covering 30 days with ≈ 3.65 days per vertical line. Figure 2 is an expanded view covering three days and 14 hours, showing a smooth profile and a flux of 230 particles $cm^{-2} s^{-1} sr^{-1} (MeV/nuc)^{-1}$ in the $5 - 7$ MeV channel (red) and 0.09 in the $138 - 200$ MeV channel (yellow). This event had a strong flare according to Fenton, Fenton, and Humble (1978), Burlaga *et al.* (1980) and Chambon *et al.* (1981), which created relativistic protons that were observed as a ground-level event (GLE) on 16 neutron monitors. The flare occurred on the rising portion of the 21st sunspot cycle, and was the first clear event for several years. The location of the source was given as N23W40 by Komori (1979) and Gombosi *et al.* (1979), who observed the event from the PROGNOZ 6 satellite, which was outside the Earth's magnetosphere at the time. The authors reported
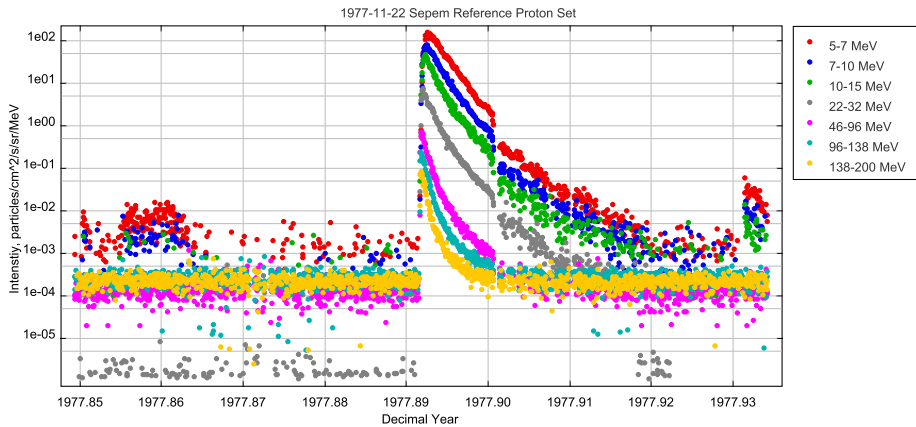
Figure 1 1977-11-22 SEP event time-intensity profile. In this image, the proton intensities are shown for the energy channels 5 – 7 MeV (red), 7 – 10 MeV (blue), 10 – 15 MeV (green), 22 – 32 MeV (gray), 66 – 95 MeV (pink), 96 – 138 MeV (cyan), and 138 – 200 MeV (yellow) for one month during November and December, 1977.

proton fluxes from 2 −500 MeV. Several authors reported that the time intensity variations of the SEPs during the event could be described by a simple diffusion model, mainly because this event took place during quiet conditions in the IMF and low solar particle background. One reason for the choice of this event is that it occurred during the short time period 1976 – 1979 when both HELIOS 1 and 2 were in operation. At this time, HELIOS 1 was at a solar ecliptic (SE) longitude of 18.3° at a distance of 0.64 AU, and HELIOS 2 was at 48.7° SE longitude at a distance of 0.58 AU from the Sun, as calculated according to http://omniweb.gsfc.nasa.gov/coho/helios/heli.html. The relative positions of the two spacecraft with Earth in the solar ecliptic frame are shown in the small diagram at the bottom of the GOES time-intensity plot of Figure 2.

The spectral plots for this event are shown in a montage in Figure 3, where each panel corresponds to a one-hour accumulation time that falls within one of the intervals delimited by vertical lines in Figure 2. In the montage the spectra for HELIOS 1 and 2 (instruments E6 and E7) and IMP-8 (instruments CRNC and GME) are plotted at subsequent times going from left to right, top to bottom. The time for each image is given at the bottom in bold type. For example, the time frame in the first plot is 1977112208 to 1977112209 or one hour, together with the date/time format of yyyymmddhh, with yyyy being the year, mm the month, dd the day, and hh the hour on a 24 hour clock. This plot represents the background intensity. The second plot is 1977112209 to 1977112210, one hour later, and represents the first change in the spectra above the background spectra. This would put this image at segment No. 2 of the time–intensity plot of Figure 2, at the beginning of the flux enhancement or the onset of the SEP event at 11:00. The peak intensity spectrum for the low energies would be in segment No. 3, 1977112217 to 1977112218, panel 3.4, that is, at 18:30. We have plotted each one-hour change in the spectra in panels 2.5, 2.6, 2.7, 2.8, and 2.9, until finally jumping ahead to the last panel No. 10.5, where the spectra return more or less to the background spectrum and are all very similar. This corresponds to segment No. 10 in Figure 2 at approximately 11:30 November 25.

The spectral plots shown in the montage of Figure 3 reveal some extraordinary shifts in the energy of the particles. The first panel (No. 2.4) shows the background spectra with the HELIOS 1 E6 (black), HELIOS 2 E6 (light blue), HELIOS 2 E7 (light green),
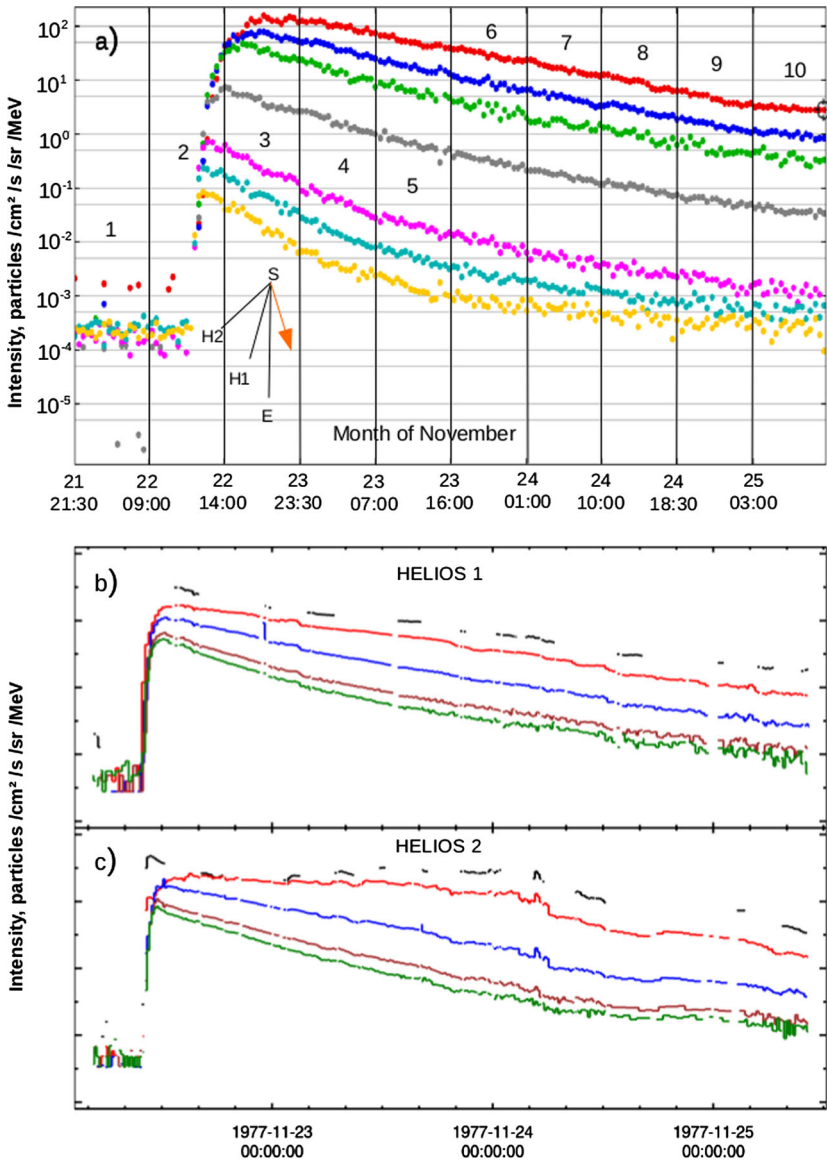
Figure 2 Time-intensity profiles of SEP protons during the 1977-11-22 event as measured by a) GOES (Crosby, Heynderickx, and Jiggens, 2013), b) HELIOS 1, and c) HELIOS 2. In this figure, the colors for the GOES plots in the top panel a) are $5-7$ MeV (red), $7-10$ MeV (blue), $10-15$ MeV (green), $22-32$ MeV (gray), $46-96$ MeV (violet), $96-138$ MeV (cyan), $138-200$ MeV (yellow), and the colors for the HELIOS 1 plots in panel b) are $1.3-3.8$ MeV (black), $3.8-12.8$ MeV (red), $12.8-26.8$ MeV (blue), $26.8-36-6$ MeV (cyan), $36.6-50.7$ MeV (green), and the colors for the HELIOS 2 plots in panel c) are $1.7-3.7$ (black), $3.6-12.6$ (red), $12.7-27.4$ MeV (blue), $27.4-37.3$ MeV (cyan), and $37.4-50.0$ MeV (green). The inset in panel a) shows the relative positions of the three spacecraft, and the orange arrow indicates the longitude of the flare associated with the event.
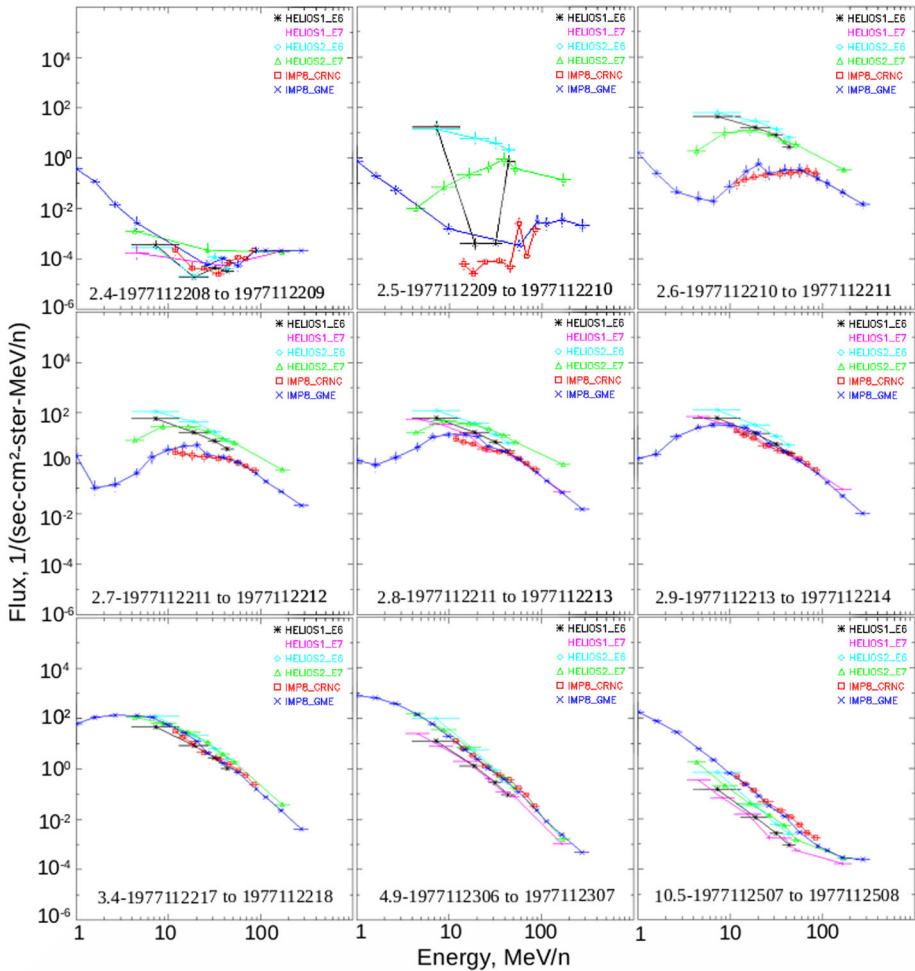
Figure 3 The time-evolution of the energy spectra of the 1977-11-22 SEP event measured at multiple spacecraft. The decimal number labeling each plot corresponds to the time interval in Figure 2 a). HELIOS 1 data from E6 and E7 are plotted in black and pink, HELIOS 2 E6 and E7 data are shown in light blue and green, respectively, while IMP-8 CRNC is depicted in red and IMP-8 GME in blue.

IMP-8 CRNC (red) and GME (blue) spacecraft observing approximately the same number of particles in the $7-200$ MeV energy range (with the exception of HELIOS 1 E7 data, which are missing in panels $2.4-2.7$). However, in the next panel 2.5, one hour later, which is the beginning of the onset of the flux enhancement of the event, the HELIOS spacecraft data show an increase in flux from 10^{-4} to 10^0 at all energies, but mostly in the higher energies from $20-200$ MeV/n. The strange "U" shape in the HELIOS 1 E6 spectra could be due to an instrument failure to record particles in the $20-30$ MeV range and is not considered relevant. A surge of higher energy particles is also observed in this panel from 50 to 200 MeV/n, which is of approximately a factor of 10 for the IMP-8, CRNC and GME instruments, but no particles are observed at the lower energies < 50 MeV/n. One hour later, in panel 2.6, the higher energy particles continue to increase

Figure 4 1977-11-22 to 1977-11-25 event-averaged spectra as measured by HELIOS 1 E6 (black), HELIOS 1 E7 (pink), HELIOS 2 E6 (light blue), HELIOS 2 E7 (green), IMP-8 CRNC (red), and IMP-8 GME (blue).
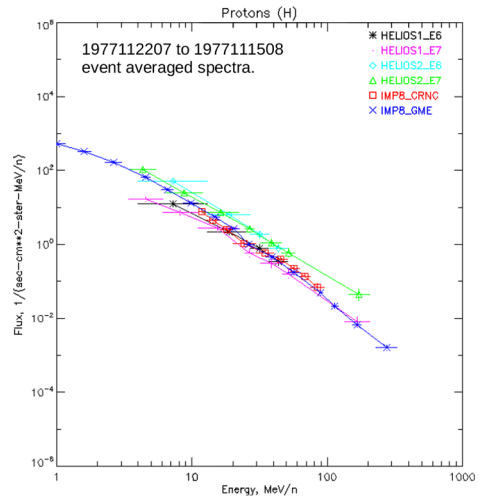
for HELIOS 1 and 2, and the lower energy particles also arrive at HELIOS and IMP-8. A surge of higher energy particles is furthermore observed at IMP-8, CRNC, and GME with no particles at the lowest energies. In the successive panels 2.7, 2.8, and 2.9, the IMP-8 higher energy particles continue to arrive, and the spectra begin to merge with those of HELIOS 1 and 2. In the IMP-8 data, the time evolution of the spectra can be described as characterized by a wave traveling along the spectra from the high to the low energies until all energy ranges are populated and the spectra take on a power-law shape. Spectra at the earlier times do not display a power law, but have an arch shape. The time it takes for the wave to travel through the spectra is ≈ 21 hours (to panel 4.9). The lowest energy particles finally begin to arrive in panel No. 3.4 at IMP-8 ≈ 9 hours after the event onset, and continue to arrive in panel No. 4.9. Panel 4.9 corresponds to the moment after the time of the peak flux enhancement. The HELIOS spacecraft seems to be better connected to the source of the event and sees higher fluxes earlier at the low energies.

For comparison with the time evolution of the spectral snapshots shown in Figure 3, the event-averaged spectrum for the three spacecraft of HELIOS 1 and 2 and IMP-8 over the whole event is shown in Figure 4, where the spectra at different locations are all very similar in a power-law shape over the energy range from 1 to 200 MeV. This shape agrees well with the spectral shape in the time evolution of the spectra in Figure 3 of panels late in the event, *e.g.* panels 4.9 and 10.5, except that the event-averaged spectrum is harder.

4.2. Bastille Day Event of 2000-07-14

The time-intensity profile for the Bastille Day event is shown in Figure 5, which is the full aspect of the month of July 2000, with only one small event before and two small events after the main particle flux increase. As reported by the LASCO[1] and HELIO[2] catalogs, the main event was the combination of a flare followed closely by a CME. The X5.7 flare started at 10:03 on July 14 (Bastille Day) at N22W07, while the CME started at 10:54 as a halo event

---

[1]See http://cdaw.gsfc.nasa.gov/index.html.
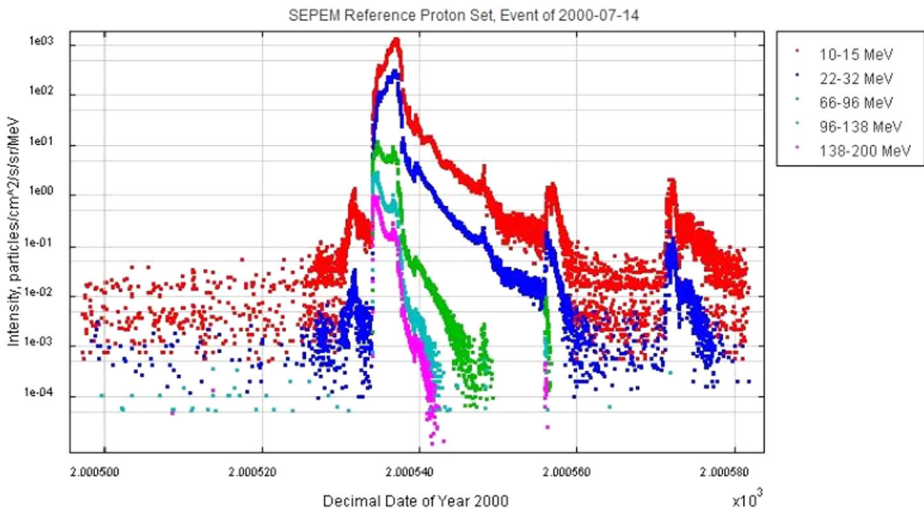
[2]See http://www.helio-vo.eu.

Figure 5 2000-07-14 SEP event time-intensity profile. In this image, the proton intensities are shown for the energy channels $10-15$ MeV (red), $22-32$ MeV (blue), $66-95$ MeV (green), $96-138$ MeV (cyan), and $138-200$ (pink) for July 2000.

with a velocity of 1674 km/s at N20W08. Together, these events were widely observed at ground level on multiple Earth-based neutron monitors, and with particle and magnetic field measurements being made directly with the WIND, ACE, and SOHO spacecraft, as reported by Belov *et al.* (2001), Klein *et al.* (2001), and Bieber *et al.* (2002). Important observations were also reported from the ULYSSES data by Zhang *et al.* (2003), at which time the spacecraft was at a distance of 3.17 AU from the Sun, and at 62° heliographic latitude and 116° longitude east of Earth. The authors reported strong fluxes of SEPs at energies > 100 MeV at both ULYSSES and Earth, and the particles observed at ULYSSES were recorded at greater intensities than expected if they had been transported along magnetic field lines alone. The authors concluded that cross-field transport was likely to be involved, otherwise ULYSSES would not have observed the particles.

The expanded profile of the Bastille Day event is shown in Figure 6 for the satellites GOES (panel a), SOHO EPHIN (panel b), SOHO ERNE (panel c), and WIND (panel d) covering a period of ≈ 4.5 days. In this profile, a shock peak at around 13:05 on July 15 is visible, after which all energies gradually decay from 10 to 200 MeV. GOES proton fluxes reach 10^3 particles cm^{-2} s^{-1} sr^{-1} (MeV/nuc)$^{-1}$ at $10-15$ MeV and 1 at $138-200$ MeV, which is a very strong particle event. SOHO ERNE protons reach a peak flux of 10^2 in the $8.1-10$ MeV channel, whereas the EPHIN instrument protons reach what could be a flux of 10^3 flux at lower energy channels from $4.3-7.8$ MeV (the instrument was blind during the onset of the event). Like IMP-8, WIND was placed in a halo orbit at L1 and should have recorded similar fluxes to GOES and SOHO, except for the fact that in 2000 NASA moved WIND into various L2 positions ≈ 1.5 – 2.0 million miles on the far side of Earth away from the Sun in the magnetotail. This would explain the much lower fluxes observed in the keV ranges. This flare and its associated CME is not related to a single active region according to Wang *et al.* (2006), who reported that the activation and eruption of a huge trans-equatorial filament preceded the flare and CME, and that many tens of halo-CMEs are found to be associated with trans-equatorial filaments and their magnetic environments. According to the authors, this could shed new light on CME magnetism.
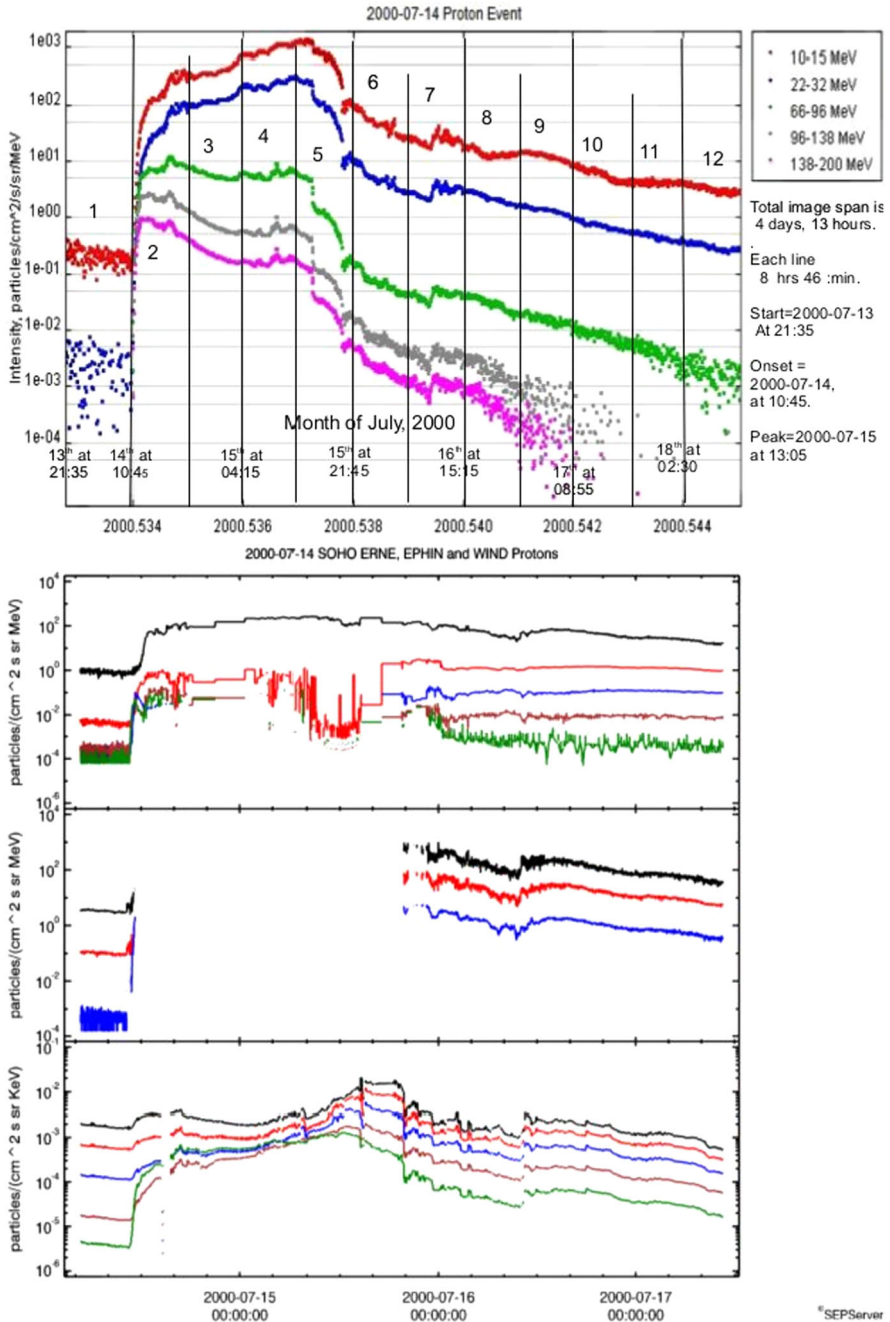
Figure 6 2000-07-14 SEP event time-intensity profiles as measured by GOES, top panel a) 10 – 15 MeV (red), 22 – 32 MeV (blue), 66 – 95 MeV (green), 96 – 138 MeV (gray), 138 – 200 (violet); SOHO EPHIN panel b) 4.3 – 7.8 MeV (black), 7.8 – 25 MeV (red), 25 – 40.9 MeV (blue), 40.9 – 53 MeV (brown); SOHO ERNE panel c) 8.1 – 10 MeV (black), 21 – 28 MeV (red), 40 – 51 MeV (blue), 64 – 80 MeV (brown), 101 – 131 MeV (green), and WIND panel d) 429 – 676 keV (black), 676 – 1360 keV (red), 1360 – 2787 keV (blue), 2787 – 6092 keV (brown), 6093 – 7087 keV (green).
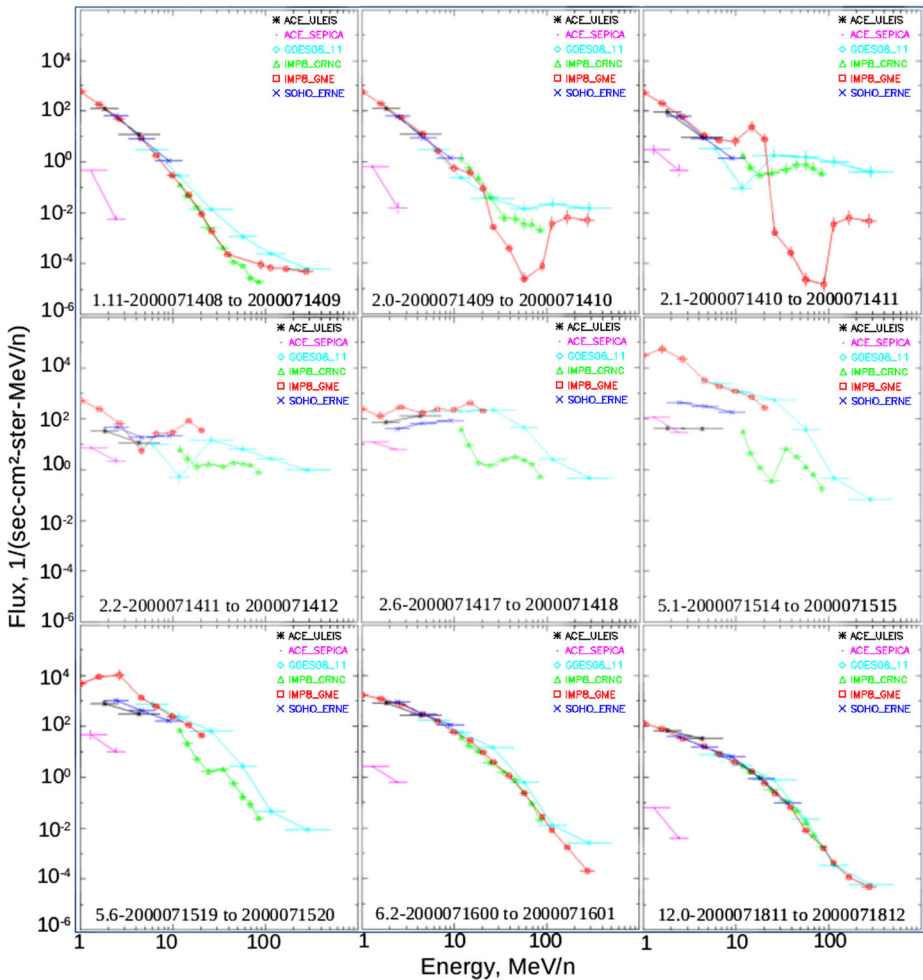
Figure 7 The time evolution of the energy spectra for the SEP event of 2000-07-14 measured at multiple spacecraft. The decimal number labeling each plot corresponds to the time interval in Figure 5 a). ACE ULEIS data are shown in black, SEPICA in pink, GOES 11 in light blue, IMP-8 CRNC in green, GME in red, and SOHO ERNE in blue.

The spectral properties of the Bastille Day events were studied by Bombardieri *et al.* (2006) using spectral fits to the spacecraft and neutron monitor data. A spectral knee was observed by Wang and Wang (2005), which occurred at > 30 MeV over an energy range from 1 to 500 MeV. The energy spectra of Fe for this event were very different from other species according to Tylka *et al.* (2001a,b), which the authors explained to be due to a two-component source population from the flare and CME. The authors stated that the five-percent admixture of flare remnants has an effect on the event-to-event variability of SEPs in large gradual SEP events, but the predominant accelerator is the CME shock.

The energy spectra of the Bastille Day event of 2000-07-14 are shown in the Figure 7 montage in a similar manner to the event of 1977-11-22, with each panel in the montage corresponding to the vertical lines delimited in Figure 6 (8 hours 46 minutes between lines).

The montage gives the spectral plots versus time for ACE, ULEIS, and SEPICA, GOES 11, IMP-8, CRNC, and GME, and SOHO ERNE. In the first panel (No. 1.11), the background flux is shown, which would be as in segment No. 1 of Figure 6. As these are all near-Earth spacecraft, the spectra would be expected to exhibit similar behavior. In the next panel, the onset of the flux enhancement of the event one hour later, we see the high energy particles arrive at GOES in the $60 - 200$ MeV/n energy range, and $50 - 90$ MeV energy range at IMP-8 CRNC, and $90 - 200$ MeV/n at IMP-8 GME. Unfortunately, SOHO ERNE is missing data in this and the remaining panels (except for the last panel No. 13.1) at the high energies, but no particles are observed at this time at the lower < 10 MeV/n energy range. One hour later in panel 2.1, we see a strange increase in the mid-range energies from $10 - 30$ MeV/n at IMP-8 GME, with no increase at the other energies, creating a Z-shaped spectrum. The higher energy particles of GOES 11 and IMP-8 CRNC continue to increase from the background rate of $10^{-5} - 10^{-4}$ to 10^0, with no particles arriving at the lower energies for all spacecraft apart from *ACE SEPICA*. In the next panel, No. 2.2, the higher energy channels of IMP-8 GME are not available, and so we will not know whether the Z shape would have persisted. However, we still have the higher energies up to 95 MeV for IMP-8 CRNC, which serve as a proxy for the loss of the GME data. There is very little change compared with panel 2.1 in the spectra for all the spacecraft in this panel, which is just three hours after the onset. After a further six hours, shown in panel No 2.8, the lower energy particles begin to arrive at the $3 - 10$ MeV/n range for all spacecraft. IMP-8 CRNC shows an S shape at the $15 - 90$ MeV/n energy range as a result of low-energy particles arriving at the $10 - 20$ MeV range. At ≈ 29 hours after the onset of this event, there is a huge surge of low-energy particles in panel 5.1, which reach a flux of 6×10^4 at IMP-8 GME, which is the peak flux for the lower energies and is associated with the passage of the interplanetary shock in segment 5 of Figure 6. The remaining three panels 5.6, 6.2, and 13.1 are the decay phase of this event, with the spectra of all spacecraft becoming very similar except for those from ACE SEPICA, which return to a particle flux similar to its observed background levels. Once again, we see the wave-like pattern in the spectra rising up at the higher energies from the onset of the event flowing up to the lower energies, and an "arch" structure in panel 2.8. It has taken ≈ 29 hours for the lower energy particles to reach peak intensities.

It is clear that the very high particle fluxes during the Bastille Day events posed a challenge to many of the instruments. Instrumental effects are the likely cause of the large differences in the spectra measured at the near-Earth spacecraft.

The event-averaged spectra for ACE, GOES, IMP-8, and SOHO over 4.5 days from 2000-07-14 at 08:00 hours to 2000-07-19 at 19:00 hours are shown in Figure 8. The spectra at the different locations show significant differences, unlike the event of 1977-11-22. This could be due to the late arrival of the low-energy particles in the $1 - 10$ MeV range approximately 34 hours after the higher energy particles in the $10 - 200$ MeV range, which is only eight hours for the 1977-11-22 event.

4.3. Event of 2001-04-15

The event of 2001-04-15 took place during a period of intense solar activity that produced at least four SEP events over the space of about three weeks from April 1, 2001, as shown in Figure 9. The event of interest is the third peak in the figure, which is expanded in Figure 10 and covers a period of about 3.63 days. The CDAW and HELIO catalogs show that these four events are caused by halo CMEs taking place on April 2, 10, 15, and 18, but the CME of interest is the one listed on April 15, 2001.

The *International Space Station* (ISS) observed two SEP events that were reported by Johnson *et al.* (2006) during the week of April 15 (there was only one event that week on

Figure 8 2000-07-14 to
2000-07-19 event-averaged
spectra as measured by ACE
ULIES (black), ACE SEPICA
(pink), GOES 11 (light blue),
IMP-8 CRNC (green), IMP-8
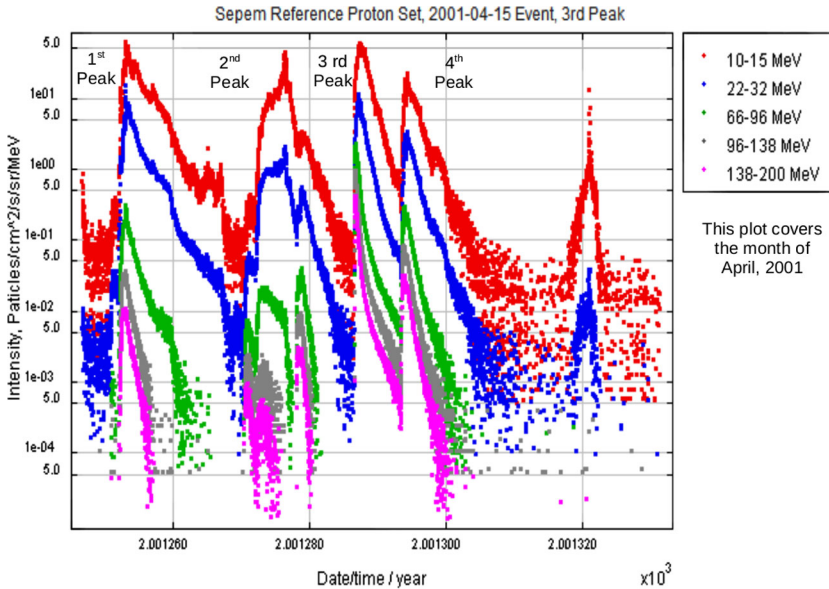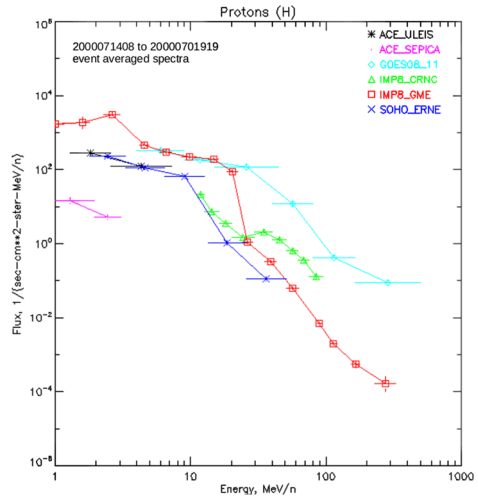GME (red), and SOHO ERNE
(blue).

Figure 9 2001-04-15 SEP event time-intensity profile. In this image, the proton intensities for four SEP events are shown for energy channels $10-15$ MeV (red), $22-32$ MeV (blue), $66-95$ MeV (green), $96-138$ MeV (gray), and $138-200$ (pink) for April, 2001. The event of interest is the third peak, which has a very high particle flux in the $138-200$ MeV energy channel.

April 15, whereas there was one on April 10 the previous week, and one on April 18 the following week), which resulted in the exposure of the crew to a record time-resolved dose of radiation. Two events were also reported by Tylka *et al.* (2002) for April 14 and 15, the second of which was thought to be associated with a flare using data from ACE, WIND, and IMP-8 covering an energy range of ≈ 30 keV/nuc to ≈ 400 MeV/nuc. Tylka and collaborators reported that these two events were the strongest impulsive and ground-level events observed in cycle 23, having come from the same active region on the Sun into similar IP
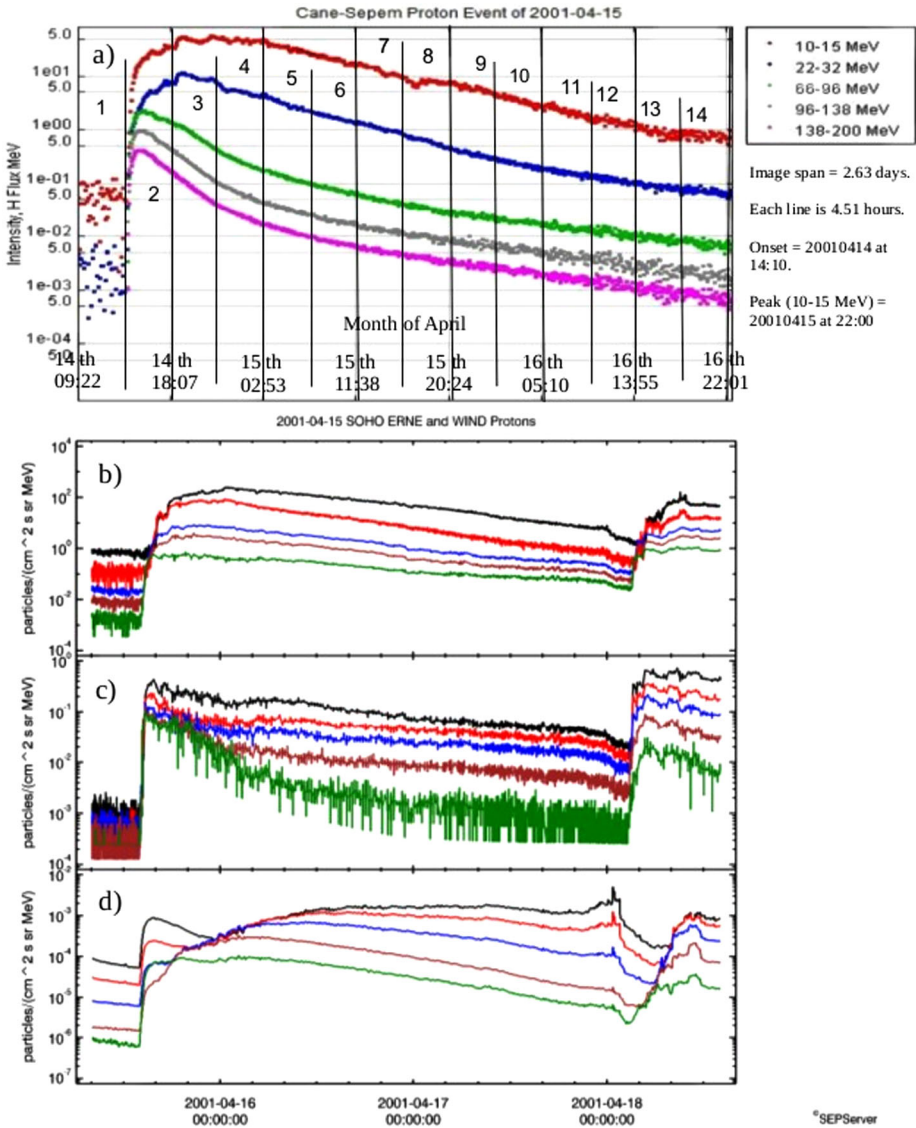
Figure 10 2001-04-15 SEP event time-intensity profile as measured by GOES, top panel a) $10-15$ MeV (red), $22-32$ MeV (blue), $66-95$ MeV (green), $96-138$ MeV (gray), $138-200$ (violet); SOHO ERNE panel b) $4.3-7.8$ MeV (black), $10-13$ MeV (red), $17-22$ MeV (blue), $21-28$ MeV (brown), $32-40$ MeV (green); SOHO ERNE panel c) $40-51$ MeV (black), $51-67$ MeV (red), $64-80$ MeV (blue), $80-101$ MeV (brown), $101-131$ MeV (green); WIND panel d) $429-676$ keV (black), $676-1360$ keV (red), $1360-2787$ keV (blue), $2787-6092$ keV (brown), and $6093-7087$ keV (green). The data of the SOHO and WIND spacecraft extend into the fourth peak of Figure 9 or an about 1.5 days longer time than for the GOES data. The small peak in panel d) at about 2001-04-18 00:00:00 might be attributed to energetic storm particles (ESPs) according to Huttunen-Heikinmaa and Valtonen (2009), since the intensity enhancements at several energy channels take place with no velocity dispersion in the vicinity of a shock passage.

space conditions. They associated the two distinctly different events with a large western longitude flare and a fast-moving CME.

This view was also supported by Rujiwarodom *et al.* (2003), who reported that the IP transport of the events was diffusive. Particle acceleration began at 13:42 UT (when observed as a GLE on neutron monitors) at the peak of the flare emissions and also at the onset of the shock-related emissions of Type II and IV radio bursts, supporting the view that a CME and not a flare was responsible for the relativistic ion acceleration. Additional support for the view of a CME/flare combination comes from Gopalswamy *et al.* (2003), who compared the two events of April 14 and 15. The authors reported that the weak event of April 14 was associated with a 830 km/s CME, while the strongest event of Cycle 23 on April 15 (the third peak of Figure 9) was associated with a faster 1200 km/s CME and X14.4 flare.

This event was also widely observed at ground level by the neutron monitoring network. Relativistic protons were reported by Muraki *et al.* (2008) to have resulted in a GLE, while GOES 10 measured the proton flux directly. It was also reported by the IPS Radio and Space Service and described by D'Andrea and Poirier (2003) as a rare X14 flare at 1 AU from the Sun originating from coordinates S20W85. The authors mentioned that only 16 flares of GOES class +X10 or larger were reported from the 22-year period between 1976 and 1998. Other interesting observations were reported by Maia *et al.* (2007) from the Nançay radioheliograph, which observed fast-moving loops in images taken in the $164 - 432$ MHz range, tracking them from $0.1 - 2.5$ solar radii above the limb of the Sun. These authors also reported white-light images from the *Large Angle Spectrometric Coronagraph* (LASCO) onboard the SOHO spacecraft. In addition, the authors reported that the event was well associated with an energetic electron event observed by the *Electron, Proton, and Alpha Monitor* (EPAM) onboard the ACE satellite.

The spectra for this event are shown in the montage in Figure 11, beginning with panel No. 1.4, which represents the background flux for this event. This is a relatively high background flux of 10^{-1} for the $10 - 15$ MeV energy channel resulting from the decay of the previous event and masking the onset at the low energies. One hour later in the next panel No. 1.5, we see the onset of the flux enhancement, with the higher energy particles > 10 MeV/n arriving at all spacecraft (ACE ULEIS/SEPICA, GOES 11, IMP-8 CRNC/GME, and SOHO ERNE). In the next panel No. 2.2, two hours later, all spacecraft continue to record further increases in the higher energy particles, with little sign of the arrival of the lower energy particles < 10 MeV/n. A wave-like spectral shape is beginning to emerge in panel 3.1, approximately five hours after the onset of the event, with a decrease in the particles recorded at the highest energies while increasing through the mid-range of energies, and with little or no increase at the lowest energies. By panel No. 3.2 one hour later, the wave-like shape and arch structure of the spectra is now more pronounced, with a further increase in flux at the mid-range of energies while remaining constant at the lowest and highest energies. The time of the peak intensity at ≈ 10 MeV for this event is in the fourth segment of panel 4.2, which is 11 hours after the onset of the event, with particles now arriving at the lowest energies. In panel 6.5 the wave-like pattern completes its propagation, and the spectrum takes on an approximately power-law shape. In the remaining two panels 10.2 and 14.4, we see the decay phase of the event, with spectra becoming very similar to each other and the flux returning to close to the background rate before the onset of the next event. All spacecraft are equally well connected to the magnetic field lines, as would be expected for their near-Earth positions. Once again, we observe the wave-like pattern of the spectra evolving from the highest energies and flowing up the slopes of the spectral curves to the lowest energies. The delay in the arrival of the lowest energy particles of 11 hours after the onset of the flux enhancement could mean an excess of high-energy particles.
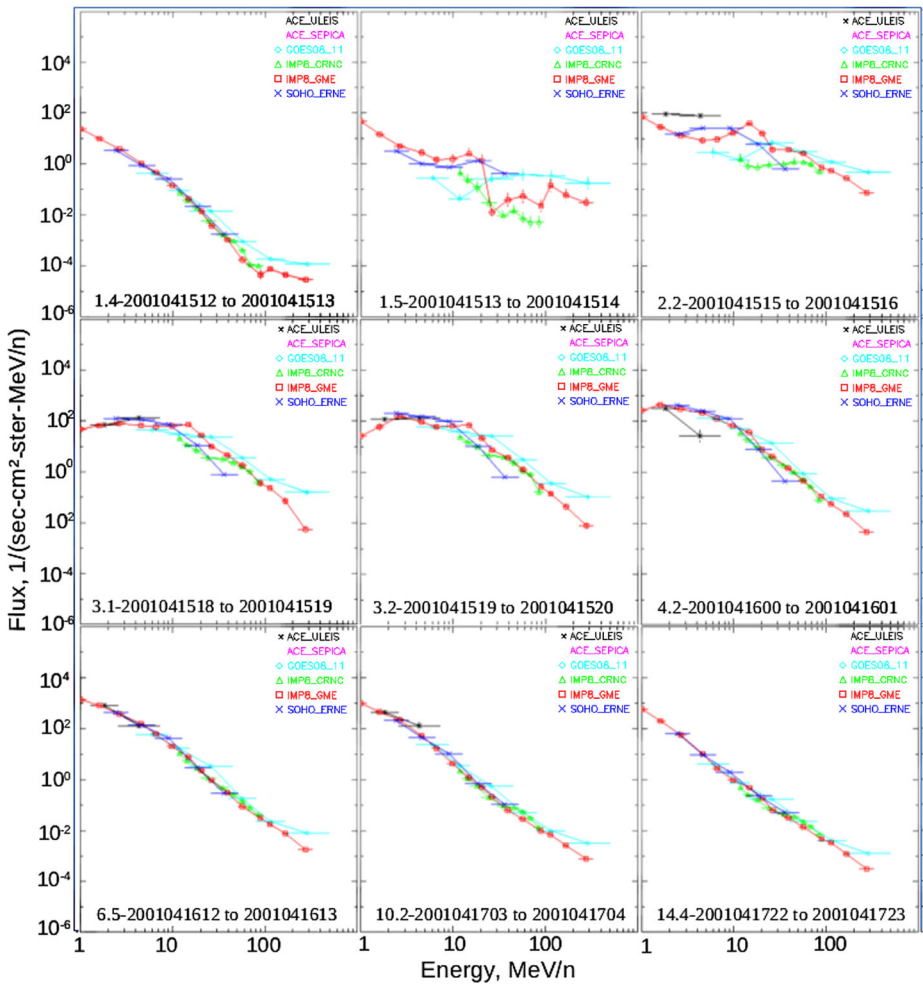
Figure 11 Time evolution of the 2001-04-15 event energy spectra measured at multiple spacecraft. The decimal number labeling each plot corresponds to the time interval in Figure 10. ACE ULEIS data are shown in black, SEPICA in pink, GOES 11 in light blue, IMP-8 CRNC in green, GME in red, and SOHO ERNE in blue.

The event-averaged spectrum for ACE, GOES, IMP-8, and SOHO over 5.5 days from 2000-07-14 at 08:00 hours to 2000-07-19 at 19:00 hours is shown in Figure 12, where the spectra are all very similar in a power-law shape over the energy range from 1 to 300 MeV. This spectrum resembles the event of 1977-11-22 in Figure 4, where the spectrum is very similar but harder than the spectral snapshots later in that event. In this event, the lower energy particles arrive only six hours after the higher energy particles, compared to eight hours for the 1977-11-22 event.

4.4. Event of 2012-03-07

The event on March 3, 2012 is a STEREO-era SEP event, which is associated with a very active solar phase at NOAA region 11429. Liu *et al.* (2014) reported a series of flares and

Figure 12 2001041512 to
2001041524 event-averaged
spectra as measured by ACE
ULIES (black), ACE SEPICA
(pink), GOES 11 (light blue),
IMP-8 CRNC (green), IMP-8
GME (red), and SOHO ERNE
(blue).
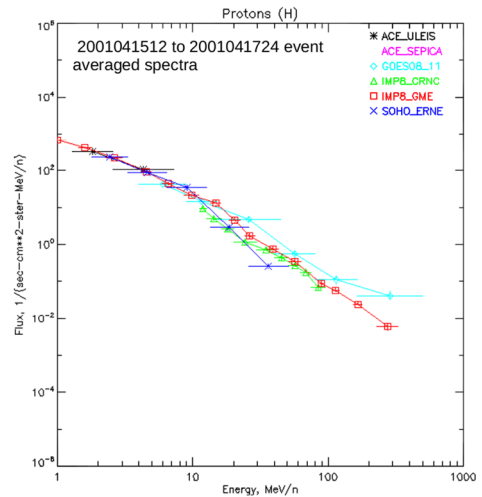
CMEs that produced a cluster of shocks and transient streams that interacted with one an-
other and resulted in a large merged interaction region (MIR) with a preceding shock. Details
from the CDAW and HELIO catalogs show that the SEP event was associated with a halo
CME at N22E12 with a velocity of 2684 km/s beginning at 00:24, and with an associated
flare of X5.4 class from the same active region (possibly at N17E15) following at 02:00. The
positions and orbital trajectories of the STEREO A and B spacecraft relative to near-Earth
and the flare direction on the Sun are shown in Figure 13, where the separation between the
two STEREO spacecraft is 132.7°.

The time-intensity profile for the GOES 13 near-Earth spacecraft is shown in Fig-
ure 14 as peak A, beginning at a relatively high background flux of 4×10^{-1} parti-
cles $cm^{-2} s^{-1} sr^{-1} (MeV/nuc)^{-1}$ in 10 to 15 MeV channel. The event shows a strong flux
of 600 particles $cm^{-2} s^{-1} sr^{-1} (MeV/nuc)^{-1}$ in the $10-15$ MeV energy channel and 0.2 par-
ticles in the $138-200$ MeV energy channel. The small hump before peak A is reported by
the SOHO LASCO CME catalog as being associated with two small C to M class events
at N16E30 and N19E32, respectively. The expanded profile for this event is shown in Fig-
ure 15, giving profiles for GOES 13 panel a, STEREO A HET panel b, and STEREO B HET
panel c. The time axes for the STEREO A and B plots are synchronized with the GOES plot,
so that the segmented lines in the GOES plot apply to them as well. These numbered seg-
ments refer to the numbered panels of the spectra in Figure 17. The time-intensity profiles
show that STEREO A is not as well connected to the magnetic field lines, but the profile is
recognizable and similar to GOES, whereas STEREO B observes a strong flux of between
5 and 100 particles $cm^{-2} s^{-1} sr^{-1} (MeV/nuc)^{-1}$ in the 60 to 100 MeV and 13.6 to 15.1 MeV
energy channels, respectively. The lower energy profiles for STEREO A and B using the
LET instrument are shown in Figure 16, where again STEREO A is not well connected to
the magnetic field lines, but STEREO B registers very high flux between 200 and 1000 par-
ticles $cm^{-2} s^{-1} sr^{-1} (MeV/nuc)^{-1}$ in the $10-12$ MeV and $4.0-4.5$ MeV energy channels,
respectively.

The event of 2012-03-07 is an interesting multi-spacecraft observed SEP event related to
a series of CMEs and flares from the same active region on the Sun. It was well observed
by GOES 13, SOHO ERNE, STEREO B (and to a lesser extent, STEREO A), and also in
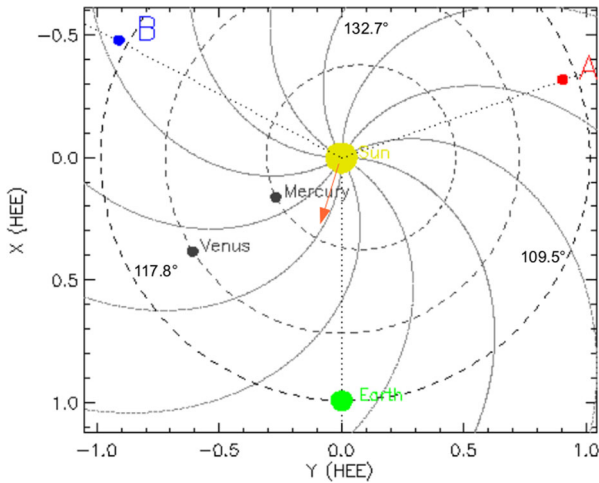the ACE low energy channels. It has a shock-associated sharp spike in the flux at the lower

Figure 13 Positions and orbital trajectories of STEREO A and B during SEP event of 20012-03-07. In the figure, the Y(HEE) and X(HEE) axis are the heliocentric Earth ecliptic along the *X*- and *Y*-axis of the Earth–Sun line, and the *Z*-axis is the ecliptic north pole. The STEREO A (ahead of Earth) spacecraft is the red circle at 0.957136 AU, the Earth's orbit is the dashed circle, and the STEREO B (behind Earth) spacecraft is the blue circle at 1.02973 AU. Earth is shown as the green circle, and the orange arrow is the position and direction of the flare. The separation angle with Earth for STEREO A is 109.5°, and for STEREO B it is 117.8°, with the separation angle between A and B being 132.7°. Light travel times to Earth are 13.2 min for A and 14.4 min for B.
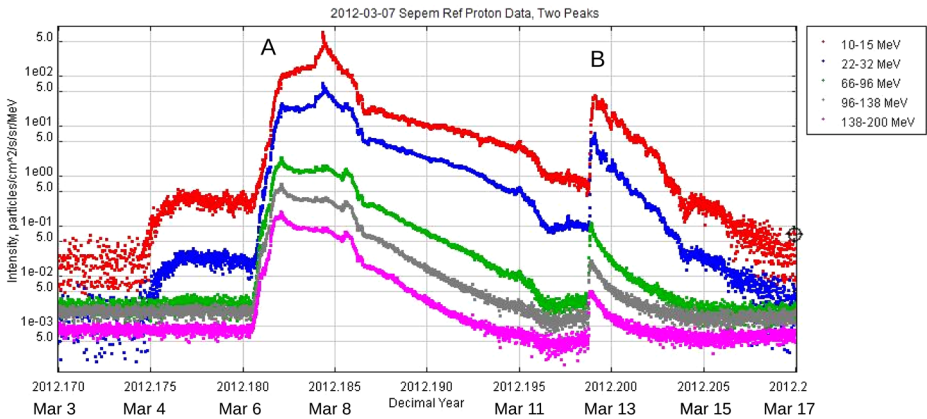

Figure 14 2012-03-07 time-intensity profile. This image is a near-Earth plot of the SEPEM GOES data for the proton intensities for two SEP events for energy channels $10-15$ MeV (red), $22-32$ MeV (blue), $66-95$ MeV (green), $96-138$ MeV (gray), and $138-200$ (pink) for March 2012. The event of interest is peak A, which has a sharp shock spike at the lower energies (red and blue plots) at 2012-03-08 at 11:15.

energy channels of $10-15$ MeV/n and $22-32$ MeV/n, but the remaining higher energy channels are close to the classic profile for an SEP event.

A montage of images for the evolution of the spectra versus time is shown in Figure 17, where the panels are numbered according to the vertical segments in the profile view of Figure 15. Beginning with panel 1.1, segment 1, the spectra of the background flux is shown.
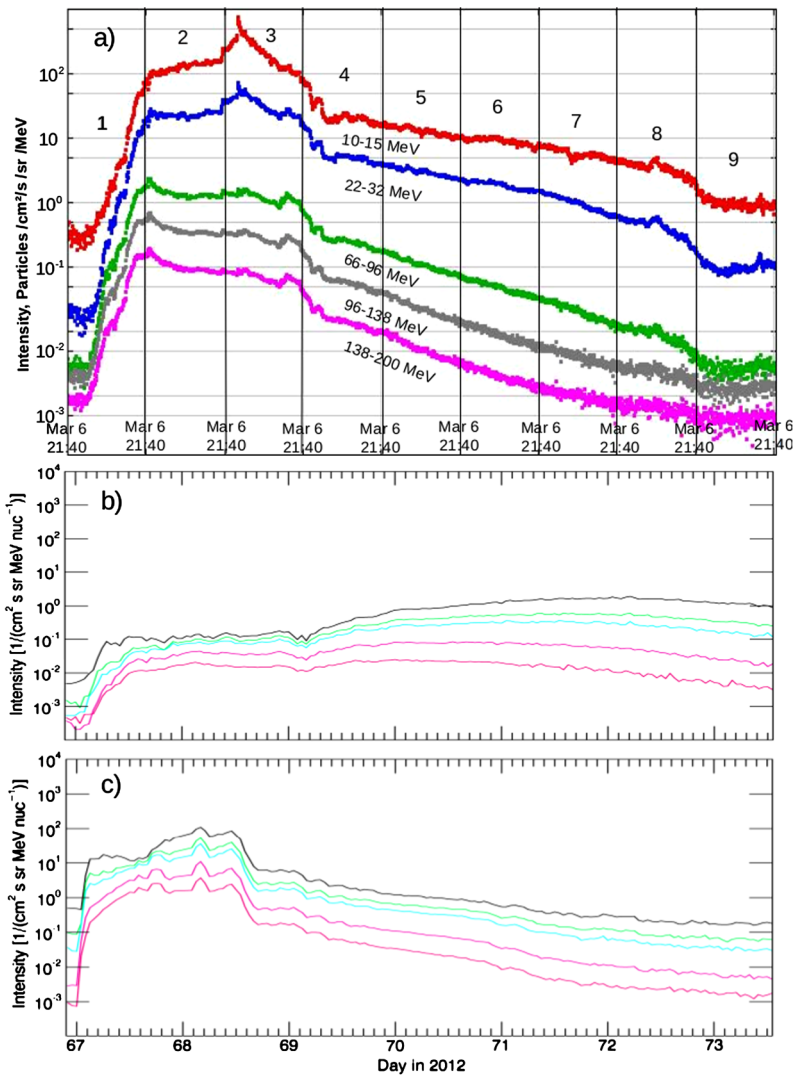
Figure 15 2012-03-07 time-intensity profiles for GOES, top panel a) $10-15$ MeV/n (red), $22-32$ MeV/n (blue), $66-95$ MeV/n (green), $96-138$ MeV/n (gray), $138-200$ MeV/n (violet); STEREO A HET panel b) $13.6-15.1$ MeV/n (black), $14.9-29.1$ MeV/n (5 green lines), $29.5-33.4$ MeV/n (blue), $33.4-35.8$ MeV/n (light blue), $35.5-40.5$ MeV/n (first pink), $40-60$ MeV/n (second pink), $60-100$ MeV/n (last pink line); STEREO B HET panel c), plotted in similar colors and energy channels as STEREO A HET.

One hour later, in panel 1.2, segment 1, we show the beginning onset of the flux enhancement of the event, where STEREO B HET is the first to observe any particles at the higher energies. In panel 1.3, GOES 13 begins to observe particles in the $138-200$ MeV energy channels, while the STEREO B flux continues to increase. As yet, there is no response from SOHO, STEREO A, or ACE. In panel 1.6 (six hours after the onset and about one-third along segment 1), we see a strong increase in flux in GOES 13 at the higher energies from $10-200$ MeV, and SOHO and STEREO B now begin to observe particles at the > 10 MeV/n energies. The ACE spacecraft also records a weak increase in flux at the lower energies of

Figure 16 2012-03-07 time-intensity profiles for STEREO A LET (top panel) and STEREO B LET (bottom panel) at energy channels 4.0 – 4.5 MeV/n (light blue), 5.0 – 6.0 MeV/n (violet), 6.0 – 8.0 MeV/n (first pink), 8.0 – 10.0 MeV/n (second pink), and 10.0 – 12.0 MeV/n (last pink).
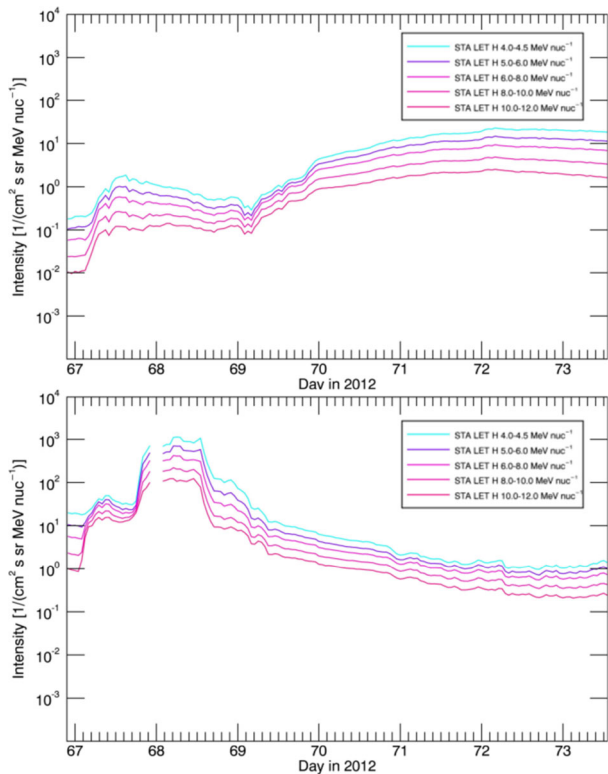
2 – 5 MeV/n. The lower energy particles now begin to arrive in panel 1.14 (14 hours after the onset, about three-fourths along segment 1), for all spacecraft, and GOES 13 now records more particle flux than STEREO B, 13 hours after the onset of the event. After about four hours in panel 2.1, segment 2, SOHO observes a drop in the higher energies and an increase in the lower energy particles that steepens the slope of the curve, as if the energy were being transferred from one to the other. In panel 3.4 ($\approx$ 36 hours after the onset) the steepening effect in the slope of the GOES 13 spectral curve is even more pronounced. This panel shows the time of the strongest flux for the lower energy particles between 10^3 and 10^4 particles cm^{-2} s^{-1} sr^{-1} (MeV/nuc)$^{-1}$, $\approx$ 34 hours after the event is in progress, with the spectra at all spacecraft becoming invariant. GOES 13 and SOHO at this point have a sort of knee shape in the 20 – 40 MeV range, with the decay of these particles lagging behind the higher energies. By panel 9.1, approximately 140 hours after the onset, the flux has decayed to the background level. As mentioned above, the background flux is relatively high at 4 $\times$ 10^{-1} particles cm^{-2} s^{-1} sr^{-1} (MeV/nuc)$^{-1}$ because this event is only one of several CMEs and flares from this active region on the Sun. Nevertheless, there is a distinct wave-like pattern and arch structure in the evolution of the spectra in a similar manner to those events observed above, and a delay of 14 hours in the arrival of the lower energy particles.

The event-averaged spectrum for ACE, GOES, SOHO, and STEREO A and B over six days from 2012-03-06 at 23:00 hours to 2012-03-12 at 20:00 hours is shown in Figure 18, where the spectra all display a power-law dependence, but show significant differences in the absolute values. These differences could be the result of the wide separation of the STEREO spacecraft away from near-Earth locations.
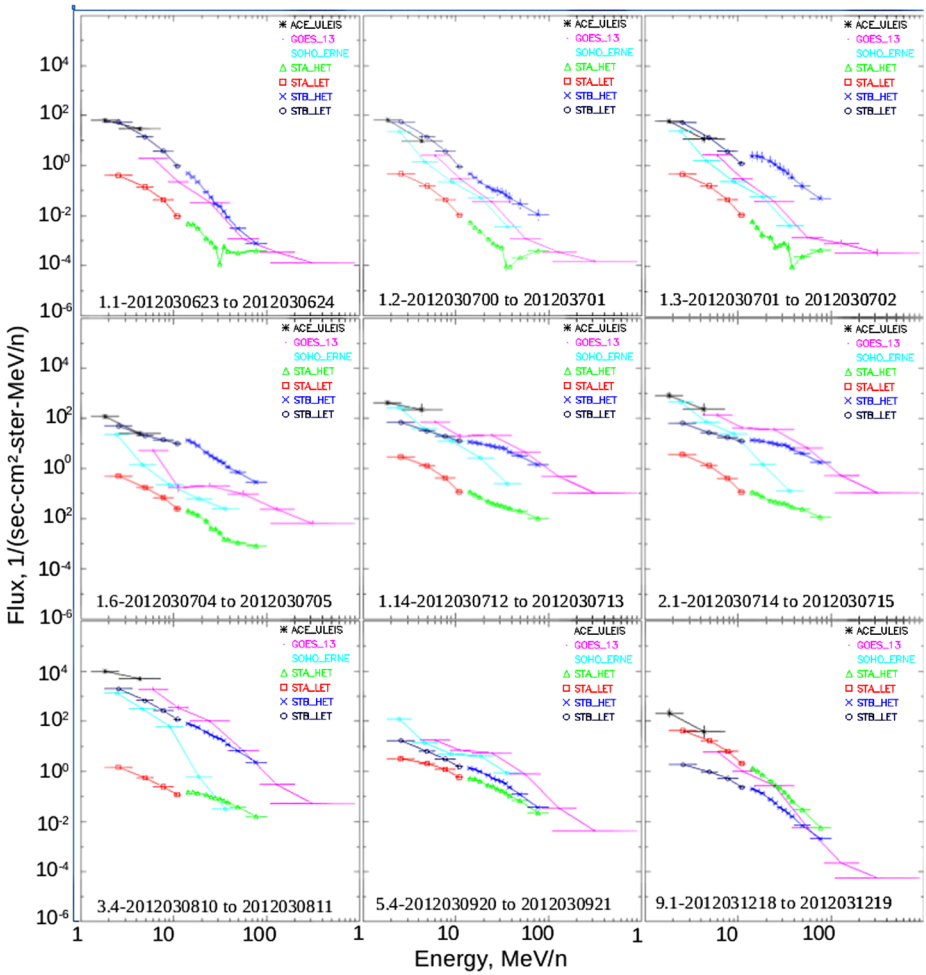
Figure 17 Time evolution of the energy spectra for event of 2012-03-07 for the five spacecraft: ACE ULEIS at $0.6 - 8.7$ MeV/n (black), GOES 11 at $0.6 - 500$ MeV/n (pink), SOHO ERNE at $1.8 - 50.7$ MeV/n (light blue); STEREO A HET at $13.6 - 100$ MeV/n (light green); STEREO A LET at $1.8 - 15.0$ MeV/n (red); STEREO B HET at $13.6 - 100$ MeV/n (blue); and STEREO B LET at $1.8 - 15.0$ MeV/n (dark gray). The numbered panels correspond to the numbered segments shown in the profiles of Figure 15, and the time frame for each panel is indicated in bold numerals below each panel.

4.5. Spectral Index Comparisons

It is interesting to compare the spectral index for high energies above 40 MeV of the event-averaged spectrum with the spectral index of a snapshot of the spectrum late in the event, as shown in Table 3. The values given here show that the event-averaged spectra at high energies are generally harder than those late in the event. "Late in the event" here refers to times when the arch-like structure previously discussed is no longer present in the spectrum, typically $\approx 20 - 43$ hours after the start of the event. The event-integrated spectra for events of 2000-07-14 and 2001-04-15 in the table were presented by Mewaldt *et al.* (2012) in the

Figure 18 2012-03-07 to 2012-03-13 event-averaged spectra as measured by ACE ULEIS (black color, GOES 13 (pink), SOHO ERNE (light blue), STA HET (green), STA LET (red), STB HET (blue), and STB LET (purple).
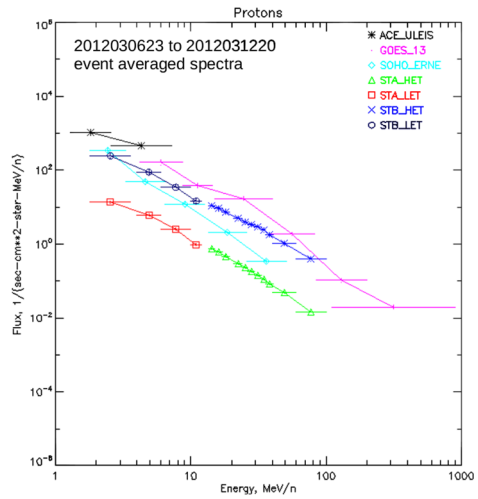

Table 3 The power law index at > 40 MeV late in the event compared to that of the event-averaged spectrum for each SEP event.

Event date	Spacecraft instruments	Power-law index after the knee	Power-law index event averaged
1977-11-22	HELIOS 1 E6	−2.84	−1.97
	HELIOS 1 E7	−2.71	−2.13
	HELIOS 2 E6	−3.67	−2.31
	HELIOS 2 E7	−3.20	−2.12
	IMP-8 CRNC	−2.83	−2.28
	IMP-8 GME	−2.79	−2.31
2000-07-14	ACE ULEIS	−1.32	−0.93
	ACE SEPICA	−3.18	−1.61
	GOES 11	−3.12	−2.28
	IMP-8 CRNC	−3.45	−2.11
	IMP-8 GME	−2.89	−3.30
	SOHO ERNE	−2.67	−2.91
2001-04-15	GOES 11	−1.78	−1.28
	ACE SEPICA	−2.39	−1.90
	IMP-8 CRNC	−2.55	−2.27
	IMP-8 GME	−2.61	−2.15
	SOHO ERNE	−2.76	−2.52
2012-03-07	ACE ULEIS	−0.98	−0.93
	GOES 13	−2.61	−2.33
	SOHO ERNE	−1.87	−2.50
	Sta HET	−2.57	−2.31
	Sta LET	−1.77	−1.77
	Stb HET	−2.32	−1.95
	Stb LET	−1.47	−1.91

energy range of 0.1 to 700 MeV. They were reported to have a double power-law form with break energies of 24 and 16 MeV, respectively.

5. Discussion and Conclusions

We presented a detailed analysis of the time evolution of the SEP spectra in four large events associated with major solar eruptive events.

Some of the common features observed in the data we presented are as follows:

- The measured spectra often show large differences at the beginning of the events. In most cases these differences arise because the spacecraft are at large distances from each other in interplanetary space. However, the spectra for spacecraft that are relatively close to each other are often discrepant (*e.g.* near-Earth spacecraft, see Figure 7). This indicates that instrumental effects may play a role, especially during very large SEP events, and also that the local solar wind and the instrument viewing direction may have an effect.
- The wave-like pattern we described in our analysis of the measured spectra, propagating from high to low energies, is a common feature of the observations. As the pattern propagates through the spectrum, the latter displays an arch shape that straightens into a power law later in the event. The typical timescale for the propagation of the wave from high to low energies is between 9 and 29 hours from the start of the event.
- The decay phase is characterized by power-law spectra that tend to become similar at far-apart locations (*cf.* invariant spectra, see Reames, Kahler, and Ng, 1997).
- Event-integrated spectra are dominated by the late-time intensities at low SEP energies and by the early-time intensities at high energies.

Several processes are expected to combine to determine the time evolution of the energy spectra as follows:

- Energy and time dependence of the particle release at the source, depending on the acceleration process.
- Particle propagation from the source to the detecting spacecraft, which is influenced by scattering processes and other phenomena that may cause transport (*e.g.* drifts, field line meandering).
- Deceleration of particles during their propagation, as a result of adiabatic deceleration *e.g.* (Ruffolo, 1995) and drift-induced deceleration (Kóta, 1979; Dalla, Marsh, and Laitinen, 2015).

Our analysis of the time evolution of the spectra does not enable us to separate the contribution of the above processes to the features of the spectra and their time variation. Modeling is required for this purpose, and we plan to carry out this type of study in the future.

References

Belov, A.V., Bieber, J.W., Eroshenko, E.A., Evenson, P., Gvozdevsky, B.B., Pchelkin, V.V., Pyle, R., Vashenyuk, V.E., Yanke, V.G.: 2001, The "Bastille Day"; GLE 14 July, 2000 as observed by the world-wide neutron monitor network. In: *International Cosmic Ray Conference* **8**, 3446. ADS.

Bieber, J.W., Dröge, W., Evenson, P.A., Pyle, R., Ruffolo, D., Pinsook, U., Tooprakai, P., Rujiwarodom, M., Khumlumlert, T., Krucker, S.: 2002, Energetic particle observations during the 2000 July 14 solar event. *Astrophys. J.* **567**, 622. ADS, DOI.

Bombardieri, D.J., Duldig, M.L., Michael, K.J., Humble, J.E.: 2006, Relativistic proton production during the 2000 July 14 solar event: the case for multiple source mechanisms. *Astrophys. J.* **644**, 565. ADS, DOI.

Burlaga, L., Lepping, R., Weber, R., Armstrong, T., Goodrich, C., Sullivan, J., Gurnett, D., Kellogg, P., Keppler, E., Mariani, F.: 1980, Interplanetary particles and fields, November 22 to December 6, 1977 – Helios, Voyager and Imp observations between 0.6 and 1.6 AU. *J. Geophys. Res.* **85**, 2227. ADS, DOI.

Cane, H.V., Reames, D.V., von Rosenvinge, T.T.: 1988, The role of interplanetary shocks in the longitude distribution of solar energetic particles. *J. Geophys. Res.* **93**, 9555. ADS, DOI.

Chambon, G., Hurley, K., Niel, M., Talon, R., Vedrenne, G., Estulin, I.V., Likin, O.B.: 1981, The November 22, 1977 solar flare – Evidence for 2.23 and 4.43 MeV line emission from the Signe 2MP experiment. *Solar Phys.* **69**, 147. ADS, DOI.

Crosby, N., Heynderickx, D., Jiggens, P.: 2013, ESA's Solar Energetic Particle Environment Modelling (SEPEM) application server, a www interface to solar energetic particle data. *ESA Contract No: 20162/06/NL/JD, Sepem reference proton data set.* http://dev.sepem.oma.be.

Crosby, N., Heynderickx, D., Jiggens, P., Aran, A., Sanahuja, B., Truscott, P., Lei, F., Jacobs, C., Poedts, S., Gabriel, S., Sandberg, I., Glover, A., Hilgers, A.: 2015, Sepem: A tool for statistical modeling the solar energetic particle environment. *Space Weather* **13**(7), 406. 2013SW001008 http://dx.doi.org/10.1002/2013SW001008. DOI.

Dalla, S., Agueda, N.: 2010, Role of latitude of source region in Solar Energetic Particle events. In: *Twelfth International Solar Wind Conference* **1216**, 613. ADS, DOI.

Dalla, S., Marsh, M.S., Laitinen, T.: 2015, Drift-induced deceleration of solar energetic particles. *Astrophys. J.* **808**, 62. ADS, DOI.

Dalla, S., Marsh, M.S., Kelly, J., Laitinen, T.: 2013, Solar energetic particle drifts in the Parker spiral. *J. Geophys. Res.* **118**(10), 5979. DOI. http://onlinelibrary.wiley.com/doi/10.1002/jgra.50589/abstract.

D'Andrea, C.P., Poirier, J.: 2003, A study of the ground level event of April 15, 2001 with GRAND. In: *International Cosmic Ray Conference* **6**, 3423. ADS.

Dresing, N., Gómez-Herrero, R., Heber, B., Klassen, A., Malandraki, O., Dröge, W., Kartavykh, Y.: 2014, Statistical survey of widely spread out solar electron events observed with STEREO and ACE with special attention to anisotropies. *Astron. Astrophys.* **567**, A27. ADS, DOI.

Fenton, A.G., Fenton, K.B., Humble, J.E.: 1978, Solar flare increase of cosmic ray intensity on November 22, 1977. *Proc. Astron. Soc. Aust.* **3**, 238. ADS.

Gombosi, I.T., Kecskeméty, N., Merényl, L., Táirallyay, M., Kurt, V.G., Logachev, Y.I., Stolpovskii, V.G., Trebukhovskaya, G.A.: 1979, Propagation of energetic particles during the November 22, 1977 event. In: *International Cosmic Ray Conference* **5**, 163. ADS.

Gopalswamy, N., Yashiro, S., Kaiser, M.L., Howard, R.A.: 2003, Coronal mass ejection interaction and particle acceleration during the 2001 April 14 15 events. *Adv. Space Res.* **32**, 2613. ADS, DOI.

Huttunen-Heikinmaa, K., Valtonen, E.: 2009, Interplanetary fast forward shocks and energetic storm particle events above 1.5 MeV. *Ann. Geophys.* **27**, 767. ADS, DOI.

Johnson, A.S., Golightly, M.J., Lin, T., Semones, E.J., Shelfer, T., Weyland, M.D., Zapp, E.N.: 2006, A comparison of measurements and predictions for the April 15 and April 18, 2001 solar proton events. *Adv. Space Res.* **37**, 1678. ADS, DOI.

Kallenrode, M.-B., Wibberenz, G., Kunow, H., Müller-Mellin, R., Stolpovskii, V., Kontor, N.: 1993, Multi-spacecraft observations of particle events and interplanetary shocks during November/December 1982. *Solar Phys.* **147**, 377. ADS, DOI.

Kelly, J., Dalla, S., Laitinen, T.: 2012, Cross-field transport of solar energetic particles in a large-scale fluctuating magnetic field. *Astrophys. J.* **750**, 47. ADS, DOI.

Klein, K.-L., Trottet, G., Lantos, P., Delaboudinière, J.-P.: 2001, Coronal electron acceleration and relativistic proton production during the 14 July 2000 flare and CME. *Astron. Astrophys.* **373**, 1073. ADS, DOI.

Komori, H.: 1979, An analysis of relativistic cosmic ray increase on 22ND November 1977. In: *International Cosmic Ray Conference* **4**, 19. ADS.

Kóta, J.: 1979, Drift – the essential process in losing energy. In: *International Cosmic Ray Conference* **3**, 13. ADS.

Laurenza, M., Consolini, G., Storini, M., Damiani, A.: 2012, A Shannon entropy approach to the temporal evolution of SEP energy spectrum. *Astrophys. Space Sci. Trans.* **8**, 19. ADS, DOI.

Li, G., Zank, G.P., Verkhoglyadova, O., Mewaldt, R.A., Cohen, C.M.S., Mason, G.M., Desai, M.I.: 2009, Shock geometry and spectral breaks in large SEP events. *Astrophys. J.* **702**, 998. ADS, DOI.

Lin, R.P., Anderson, K.A., Ashford, S., Carlson, C., Curtis, D., Ergun, R., Larson, D., McFadden, J., McCarthy, M., Parks, G.K., Rème, H., Bosqued, J.M., Coutelier, J., Cotin, F., D'Uston, C., Wenzel, K.-P.,

Sanderson, T.R., Henrion, J., Ronnet, J.C., Paschmann, G.: 1995, A three-dimensional plasma and energetic particle investigation for the wind spacecraft. *Space Sci. Rev.* **71**, 125. ADS, DOI.

Liu, Y.D., Richardson, J.D., Wang, C., Luhmann, J.G.: 2014, Propagation of the 2012 March coronal mass ejections from the sun to heliopause. *Astrophys. Lett. Commun.* **788**, L28. ADS, DOI.

Maia, D.J.F., Gama, R., Mercier, C., Pick, M., Kerdraon, A., Karlický, M.: 2007, The radio-coronal mass ejection event on 2001 April 15. *Astrophys. J.* **660**, 874. ADS, DOI.

Marsh, M.S., Dalla, S., Kelly, J., Laitinen, T.: 2013, Drift-induced perpendicular transport of solar energetic particles. *Astrophys. J.* **774**, 4. ADS, DOI.

McCuistion, D., Bengston, C.: 1996, GOES-8 and 9 mission launch and operations support overview. In: Guyenne, T.-D. (ed.) *Space Mission Operations and Ground Data Systems – SpaceOps '96*, *ESA Special Publication* **394**, 76. ADS.

Mewaldt, R.A., Cohen, C.M.S., Cook, W.R., Cummings, A.C., Davis, A.J., Geier, S., Kecman, B., Klemic, J., Labrador, A.W., Leske, R.A., Miyasaka, H., Nguyen, V., Ogliore, R.C., Stone, E.C., Radocinski, R.G., Wiedenbeck, M.E., Hawk, J., Shuman, S., von Rosenvinge, T.T., Wortman, K.: 2008, The Low-Energy Telescope (LET) and SEP central electronics for the STEREO mission. *Space Sci. Rev.* **136**(1 – 4), 285. DOI. http://link.springer.com/article/10.1007/s11214-007-9288-x.

Mewaldt, R.A., Looper, M.D., Cohen, C.M.S., Haggerty, D.K., Labrador, A.W., Leske, R.A., Mason, G.M., Mazur, J.E., von Rosenvinge, T.T.: 2012, Energy spectra, composition, and other properties of ground-level events during solar cycle 23. *Space Sci. Rev.* **171**, 97. ADS, DOI.

Muraki, Y., Matsubara, Y., Masuda, S., Sakakibara, S., Sako, T., Watanabe, K., Bütikofer, R., Flückiger, E.O., Chilingarian, A., Hovsepyan, G., Kakimoto, F., Terasawa, T., Tsunesada, Y., Tokuno, H., Velarde, A., Evenson, P., Poirier, J., Sakai, T.: 2008, Detection of high-energy solar neutrons and protons by ground level detectors on April 15, 2001. *Astropart. Phys.* **29**, 229. ADS, DOI.

Onsager, T., Grubb, R., Kunches, J., Matheson, L., Speich, D., Zwickl, R.W., Sauer, H.: 1996, Operational uses of the GOES energetic particle detectors. In: Washwell, E.R. (ed.) *GOES-8 and Beyond*, *Society of Photo-Optical Instrumentation Engineers (SPIE) Conference Series* **2812**, 281. ADS, DOI.

Porsche, H.: 1981, HELIOS mission: Mission objectives, mission verification, selected results. In: Burke, W.R. (ed.) *Solar System and Its Exploration*, *ESA Special Publication* **164**, 43. ADS.

Reames, D.V., Barbier, L.M., Ng, C.K.: 1996, The spatial distribution of particles accelerated by coronal mass ejection-driven shocks. *Astrophys. J.* **466**, 473. ADS, DOI.

Reames, D.V., Kahler, S.W., Ng, C.K.: 1997, Solar energetic-particle spectra and the structure of coronal mass ejections. In: *International Cosmic Ray Conference* **1**, 185. ADS.

Richardson, I.G., von Rosenvinge, T.T., Cane, H.V., Christian, E.R., Cohen, C.M.S., Labrador, A.W., Leske, R.A., Mewaldt, R.A., Wiedenbeck, M.E., Stone, E.C.: 2014, > 25 MeV proton events observed by the High Energy Telescopes on the STEREO A and B spacecraft and/or at Earth during the first ∼ seven years of the STEREO mission. *Solar Phys.* **289**(8), 3059. DOI. http://link.springer.com/article/10.1007/s11207-014-0524-8.

Ruffolo, D.: 1995, Effect of adiabatic deceleration on the focused transport of solar cosmic rays. *Astrophys. J.* **442**, 861. ADS, DOI.

Rujiwarodom, M., Bieber, J., Droge, W., Everson, P., Pyle, R., Ruffolo, D., Tooprakai, P., Khumlumlert, T.: 2003, Time of solar energetic particle acceleration on 15-04-2001. In: *IAU Joint Discussion*, *IAU Joint Discussion* **7**, 35. ADS.

Stone, E.C., Cohen, C.M.S., Cook, W.R., Cummings, A.C., Gauld, B., Kecman, B., Leske, R.A., Mewaldt, R.A., Thayer, M.R., Dougherty, B.L., Grumm, R.L., Milliken, B.D., Radocinski, R.G., Wiedenbeck, M.E., Christian, E.R., Shuman, S., von Rosenvinge, T.T.: 1998, The solar isotope spectrometer for the advanced composition explorer. *Space Sci. Rev.* **86**(1 – 4), 357. DOI. http://link.springer.com/article/10.1023/A:1005027929871.

Torsti, J., Valtonen, E., Lumme, M., Peltonen, P., Eronen, T., Louhola, M., Riihonen, E., Schultz, G., Teittinen, M., Ahola, K., Holmlund, C., Kelhä, V., Leppälä, K., Ruuska, P., Strömmer, E.: 1995, Energetic particle experiment ERNE. *Solar Phys.* **162**(1 – 2), 505. DOI. http://link.springer.com/article/10.1007/BF00733438.

Tylka, A.J., Boberg, P.R., Cohen, C.M.S., Dietrich, W.F., Maclennan, C.G., Mason, G.M., Reames, D.V., McGuire, R.E., Ng, C.K.: 2001a, Energy spectra of very large gradual solar particle events. In: *International Cosmic Ray Conference* **8**, 3189. ADS.

Tylka, A.J., Cohen, C.M.S., Dietrich, W.F., Maclennan, C.G., McGuire, R.E., Ng, C.K., Reames, D.V.: 2001b, Evidence for remnant flare suprathermals in the source population of solar energetic particles in the 2000 Bastille day event. *Astrophys. Lett. Commun.* **558**, L59. ADS, DOI.

Tylka, A.J., Boberg, P.R., Cohen, C.M.S., Dietrich, W.F., Maclennan, C.G., Mason, G.M., Ng, C.K., Reames, D.V.: 2002, Flare- and shock-accelerated energetic particles in the solar events of 2001 April 14 and 15. *Astrophys. Lett. Commun.* **581**, L119. ADS, DOI.

Vainio, R., Valtonen, E., Heber, B., Malandraki, O.E., Papaioannou, A., Klein, K.-L., Afanasiev, A., Agueda, N., Aurass, H., Battarbee, M., Braune, S., Dröge, W., Ganse, U., Hamadache, C., Heynderickx, D., Huttunen-Heikinmaa, K., Kiener, J., Kilian, P., Kopp, A., Kouloumvakos, A., Maisala, S., Mishev, A., Miteva, R., Nindos, A., Oittinen, T., Raukunen, O., Riihonen, E., Rodríguez-Gasén, R., Saloniemi, O., Sanahuja, B., Scherer, R., Spanier, F., Tatischeff, V., Tziotziou, K., Usoskin, I.G., Vilmer, N.: 2013, The first SEPServer event catalogue 68-MeV solar proton events observed at 1 AU in 1996 – 2010. *J. Space Weather Space Clim.* **3**(27), A12. ADS, DOI.

von Rosenvinge, T.T., Reames, D.V., Baker, R., Hawk, J., Nolan, J.T., Ryan, L., Shuman, S., Wortman, K.A., Mewaldt, R.A., Cummings, A.C., Cook, W.R., Labrador, A.W., Leske, R.A., Wiedenbeck, M.E.: 2008, The high energy telescope for STEREO. *Space Sci. Rev.* **136**(1 – 4), 391. DOI. http://link.springer.com/article/10.1007/s11214-007-9300-5.

Wang, R., Wang, J.: 2005, Solar relativistic proton fluxes in the solar flare of 14 July 2000. In: Dere, K., Wang, J., Yan, Y. (eds.) *Coronal and Stellar Mass Ejections*, *IAU Symposium* **226**, 381. ADS, DOI.

Wang, J.-X., Zhou, G.-P., Wen, Y.-Y., Zhang, Y.-Z., Wang, H.-N., Deng, Y.-Y., Zhang, J., Harra, L.K.: 2006, Transequatorial filament eruption and its link to a coronal mass ejection. *Chin. J. Astron. Astrophys.* **6**, 247. ADS, DOI.

Wiedenbeck, M.E., Mason, G.M., Cohen, C.M.S., Nitta, N.V., Gómez-Herrero, R., Haggerty, D.K.: 2013, Observations of solar energetic particles from ^{3}He-rich events over a wide range of heliographic longitude. *Astrophys. J.* **762**, 54. ADS, DOI.

Zhang, M., McKibben, R.B., Lopate, C., Jokipii, J.R., Giacalone, J., Kallenrode, M.-B., Rassoul, H.K.: 2003, Ulysses observations of solar energetic particles from the 14 July 2000 event at high heliographic latitudes. *J. Geophys. Res.* **108**, 1154. ADS, DOI.